Determinants of Specificity of MDM2 for the Activation Domains of p53 and p65: Proline27 Disrupts the MDM2-Binding Motif of p53[†]

Susan Carr Zondlo, Aaron E. Lee, and Neal J. Zondlo*

Department of Chemistry and Biochemistry, University of Delaware, Newark, Delaware 19716

Received February 14, 2006; Revised Manuscript Received June 29, 2006

ABSTRACT: Transcriptional activation and repression via the transcription factors p53 and p65 are mediated by hydrophobic short linear motifs (FXXΦΦ) in their activation domains (ADs). To understand the molecular basis for specificity in binding to disparate biological targets, a series of chimeric peptides was synthesized, with sequences derived from the ADs of p53, which binds both the general transcriptional machinery and the repressor protein MDM2, and p65, which is reported to bind the general transcriptional machinery but not MDM2. The FXXΦΦ motifs of p53 and p65 differ by only two residues, whereas the flanking sequences have no sequence identity. The affinities of the chimeric peptides to $MDM2_{25-117}$ and $hTAF_{II}31_{1-140}$ were determined. Specificity for binding MDM2 via FXXΦΦ motifs derives almost entirely from Trp23 of p53, with a 3.0 kcal mol^{-1} loss of binding energy when Trp23 is changed to p65-derived Leu. The identity of the N-terminal flanking sequence did not significantly affect binding to MDM2. In contrast, replacement of the C-terminal sequence of p53 with that of p65 increased the affinity of the chimera for MDM2 by 1.1 kcal mol^{-1}, contrary to expectations. Replacement of the highly conserved residue Pro27 of p53 with Ser from p65 resulted in a 2.3 kcal mol^{-1} improvement in binding to MDM2, generating a ligand (p53-P27S) (K_d = 4.7 nM) that exhibits the highest MDM2 affinity observed for a genetically encodable ligand. The basis for the increased affinity of p53-P27S over p53 was examined by circular dichroism and nuclear magnetic resonance. Pro27 disrupts the recognition α-helix of p53, with p53-P27S significantly more α-helical than p53.

Transcription from a promoter requires DNA binding by a promoter-specific transcription factor as well as by the general transcription machinery of RNA polymerase II. The activation domains (ADs)[1] of transcription factors are critical linkers between these DNA-binding events, with the AD recruiting the transcriptional machinery to the promoter to initiate transcription (*1*). The potency of ADs in binding the transcriptional machinery correlates with the extent of gene transcript produced (*2*−*5*). ADs may alternatively interact with transcriptional repressor proteins, which mask the AD and thereby block transcription (*6*−*9*). The interplay of ADs between the general transcription machinery and repressor proteins is a critical dynamic in transcription, and knowledge of the specificity of these interactions is central to our understanding of transcription at a molecular level (*10*).

p53 is a transcription factor responsive to DNA damage and other cellular insults (*6*, *11*, *12*). Activation of p53 may result in cell-cycle arrest and the upregulation of DNA-repair genes or alternatively may induce apoptosis. Thus, p53 is a central regulator preventing the replication of cells with damaged DNA. Because of this regulatory role, p53 is a critical gene that is observed to be mutated in a majority of cancers.

p53 is regulated via a feedback loop with the repressor oncoprotein MDM2 (*7*−*9*, *13*−*15*). MDM2 both binds specifically to the AD of p53, preventing transcription from p53-responsive genes, and is a ubiquitin ligase, leading to the destruction of p53 (*16*). Thus, the AD of p53 may interact with either the general transcription machinery, with the TFIID protein component $hTAF_{II}31$ an important interaction target and leading to the transcription of p53-responsive genes, or may alternatively bind to MDM2, leading to the destruction of p53 (*17*−*19*). This dynamic is central in numerous cancers, with overexpression of MDM2 commonly observed.

The interactions between p53 and MDM2 and between p53 and $hTAF_{II}31$ are mediated by short α-helices from the AD of p53 (*19*−*23*). The interaction motif of p53 undergoes a disorder-to-order transition upon binding either MDM2 or $hTAF_{II}31$, with residues of an FXXΦΦ motif (Φ = hydrophobic residue) adopting an α-helical conformation in the protein complexes (*19*, *20*, *24*). Crystallographically, Phe19, Leu22, Trp23, Leu26, and Pro27 of p53 make hydrophobic contacts with MDM2, with Trp23 deeply buried

[†] This work was supported by the NIH (1P20 RR17716-01) (NCRR). NMR instrumentation was supported by the NIH (2P20 RR016472-04) and the Kresge Foundation.

* To whom correspondence should be addressed. Telephone: +1-302-831-0197. Fax: +1-302-831-6335. E-mail: zondlo@udel.edu.

[1] Abbreviations: Θ, mean residue ellipticity; AD, activation domain; BSA, bovine serum albumin; CD, circular dichroism; CSI, chemical-shift index; DMF, *N*,*N*-dimethylformamide; DTT, dithiothreitol; EDTA, ethylenediaminetetraacetic acid; HPLC, high-performance liquid chromatography; HSQC, heteronuclear single-quantum coherence; IPTG, isopropyl-β-D-thiogalactopyranoside; $^3J_{\alpha N}$, three-bond coupling constant between the α proton and the amide proton; NMR, nuclear magnetic resonance; NOE, nuclear Overhauser effect; NOESY, nuclear Overhauser effect spectroscopy; PBS, phosphate-buffered saline solution; TES, triethylsilane; TFA, trifluoroacetic acid; TFE, trifluoroethanol; TOCSY, total correlation spectroscopy; t_R, retention time by HPLC; TSP, 3-trimethylsilylpropionate.

10.1021/bi060309g CCC: $33.50
Published on Web 09/07/2006

(*20*). The interaction between p53 and MDM2 has also been subjected to extensive functional analysis to determine the extent of the binding epitope and to identify the key residues in binding, with the hydrophobic residues, particularly Trp23, identified as critical for transcription and for binding MDM2 (*25*−*30*).

Short hydrophobic α-helical FXXΦΦ motifs have been observed in many proteins as general mediators of AD−$hTAF_{II}31$ (and more generally AD−coactivator) interactions (*19*, *21*−*23*, *31*, *32*). The protein p65 (RelA), which is a member of the NF-KB family of heterodimeric transcription factors critical in inflammation-mediated signaling and prevention of apoptosis, contains a potent AD with FXXΦΦ motifs that are functionally critical for transcriptional activation (*19*, *32*−*34*). The p65 AD has been characterized by nuclear magnetic resonance (NMR), binding assays, and functional assays as a binding partner of $hTAF_{II}31$, with the p65 AD undergoing a transition from random coil to α-helix upon binding $hTAF_{II}31$ (*19*, *22*, *32*, *33*). In these studies, Uesugi and Verdine demonstrated that MDM2 is a relatively specific protein, binding the FXXΦΦ motif of the AD of p53 but not, under the stringent conditions examined, the FXXΦΦ motifs of the ADs of p65 or VP16 (*19*). In contrast, $hTAF_{II}31$ readily bound the ADs of p53, p65, and VP16 (*19*, *21*). These critical studies provided important insight into the interactions between ADs and potential protein partners. However, in these studies, the affinities of these ADs for their binding partners were not quantified, which is necessary for a detailed understanding of specificity and to understand conditions in which binding between different partners is favored.

Because the FXXΦΦ motif plays a central role in both transcriptional activation and transcriptional repression, we sought to understand the determinants of specificity for binding to either co-activator proteins or repressor proteins. In addition, the disruption of the interaction between MDM2 and p53 has been extensively examined as an anticancer therapeutic (*10*, *13*−*15*, *35*−*37*). However, molecules capable of mimicking the p53 AD to bind MDM2 might also be expected to bind other targets of the p53 AD, including $hTAF_{II}31$, and thereby also prevent the transcription of p53-responsive genes. To address these questions, we have undertaken an examination of the residue determinants of specificity for transcriptional activation versus transcriptional repression. We examined the determinants of specificity by the preparation and analysis of chimeras of the potent AD of p65, which binds $hTAF_{II}31$, and the p53 AD, which binds both $hTAF_{II}31$ and MDM2 (*19*).

EXPERIMENTAL PROCEDURES

Protein Expression and Purification. The DNA region coding for residues 25−117 of MDM2 was amplified by polymerase chain reaction (PCR) from the plasmid pGmdm2, obtained from the lab of Hua Lu, using the following primers: 5′-taaattccatatggagaccctggttagaccaaagcca-3′ and 3′-gtcaatcagcaggaatcatcggactagggatccaatt-5′. For $hTAF_{II}31$, DNA encoding residues 1−140 was amplified by PCR from the plasmid pG31, also from the lab of Hua Lu, using the primers 5′-taaattccatatggagtctggcaagacggcttct-3′ and 3′-cagaaaaag-gcatcaacttctgcgtagggatccaatt-5′. PCR products were subcloned into the pET-14b vector (Novagen) containing an isopropyl-β-D-thiogalactopyranoside (IPTG)-inducible promoter and a HexaHis tag. The resulting plasmids were used to transform BL21(DE3)pLysS competent cells (EMD Biosciences), which were used for protein expression. Cells grown in luria broth (Fisher Scientific) overnight at 37 °C with shaking were used to seed 500 mL cultures of terrific broth (Fisher Scientific) that were then grown for 1.5 h at 37 °C. A total of 0.4 mM IPTG was added to induce protein expression, and cultures were then grown for 5 h at 30 °C with shaking. Bacterial pellets were collected by centrifugation and frozen until purification. For protein purification, His-bind resin (EMD Biosciences) was used following the instructions of the manufacturer. Protein eluents were dialyzed into phosphate-buffered saline (PBS) (pH 7.4) containing 5 mM ethylenediaminetetraacetic acid (EDTA) and 0.5 mM dithiothreitol (DTT) using a Spectra/Por 6 membrane, molecular weight cut-off (MWCO) 10 000 (Spectrum Laboratories). Purified proteins were analyzed on a 10% Tris sodium dodecyl sulfate−polyacrylamide gel electrophoresis (SDS−PAGE) gel (BioRad), and their identity was confirmed by quantitative amino acid analysis (Keck Center, Yale University, New Haven, CT). Bradford assays (BioRad) were used to determine protein concentrations.

Peptide Synthesis and Characterization. Peptides were synthesized via standard Fmoc solid-phase peptide synthesis on a CEM Liberty microwave peptide synthesizer or on a Rainin PS3 peptide synthesizer. Peptides containing a p53-derived C terminus were synthesized using Rink amide resin. Peptides containing a p65-derived C terminus were synthesized using Fmoc-Ser(O*t*Bu)-Wang resin. All peptides were acetylated on the N terminus, except $p65_{532-551}$ and phosphorylated $p65_{532-551}$.

Phosphorylated $p65_{532-551}$ was synthesized using Fmoc-Ser(OTrt)-OH at the site of serine phosphorylation and Fmoc-Ser(O*t*Bu)-OH at all other serine residues. After peptide synthesis, with the N terminus Fmoc-protected, the trityl group was selectively removed with 2% trifluoroacetic acid (TFA) and 5% triethylsilane (TES) in CH_2Cl_2 (3 × 1 min). Phosphitylation was performed under nitrogen by the addition of tetrazole (1.35 mmol; 3 mL of 3% tetrazole in acetonitrile) (Transgenomics) and *O*,*O*-dibenzyl-*N*,*N*-diisopropylphosphoramidite (500 μL, 1.52 mmol) (Fluka) to 50 mg of resin and allowed to react for 5 h with mixing. The solution was removed, and the resin was washed with *N*,*N*-dimethylformamide (DMF) (3×) and CH_2Cl_2 (3×). Oxidation was performed with *tert*-butyl hydroperoxide (3 mL of a 3 M solution in CH_2Cl_2) and allowed to react with mixing for 1 h. The solution was removed, and the resin was washed with DMF (3×) and CH_2Cl_2 (3×). Fmoc deprotection of the N terminus was achieved using 20% piperidine in DMF.

Peptides were subjected to cleavage from the resin and deprotection for 2.5−3 h (40 μL of thioanisole, 40 μL of ethanedithiol, 40 μL of phenol, 40 μL of 1 M DTT, and 1.5 mL of TFA). $p65_{532-551}$ and phosphorylated $p65_{532-551}$ were cleaved as above without DTT. TFA was evaporated with nitrogen, and the peptides were precipitated with ether. The precipitates were dissolved in 1.5 mL of 100 mM phosphate buffer (pH 8), and the resulting solution was filtered. The peptides were purified by reverse-phase high-performance liquid chromatography (HPLC) (Vydac semipreparative C18, 10 × 250 mm, 5 μm particle size, 300 Å pore). Peptides were purified to homogeneity, using a linear gradient of

0−60% buffer B (80% MeCN, 20% H_2O, and 0.05% TFA) in buffer A (98% H_2O, 2% MeCN, and 0.06% TFA) over 60 min unless otherwise indicated. The peptides 666, 333, 336, 636, and 366 were purified to homogeneity using a linear gradient of 0−60% buffer B in buffer A over 120 min. Peptide purity was indicated by the presence of a single peak on analytical HPLC reinjection (Microsorb MV C18, 4.6 × 250 mm, 3−5 μm particle size, 100 Å pore). Peptide identity was characterized by electrospray ionization−mass spectrometry (ESI−MS) in positive-ion mode on an LCQ Advantage (Finnigan) mass spectrometer. Phosphorylated $p65_{532-551}$ was characterized by ESI−MS in negative-ion mode. Observed masses of peptides for which the multiply-charged species were seen are reported as the deconvoluted molecular masses. Analytical data for the peptides: 333 [retention time by HPLC (t_R), 115.9 min; expected mass, 2371.2; observed mass, 2374.1 $(M + 2H)^{2+}$], 336 [t_R, 75.7 min; expected mass, 2065.9; observed mass, 2068.4 $(M + 2H)^{2+}$], 633 [t_R, 52.5 min; expected mass, 2338.1; observed mass, 2340.4 $(M + 2H)^{2+}$], 636 [t_R, 86.1 min; expected mass, 2032.8; observed mass, 2035.6 $(M + 2H)^{2+}$], 666 [t_R, 91.8 min; expected mass, 1915.9; observed mass, 1918.0 $(M + 2H)^{2+}$], 663 [t_R, 54.3 min; expected mass, 2221.1; observed mass, 2223.6 $(M + 2H)^{2+}$], 366 [t_R, 90.7 min; expected mass, 1948.9; observed mass, 1950.8 $(M + 2H)^{2+}$], 363 [t_R, 54.2 min; expected mass, 2254.2; observed mass, 2257.0 $(M + 2H)^{2+}$], p53-D21A [t_R, 53.6 min; expected mass, 2327.2; observed mass, 2330.4 $(M + 2H)^{2+}$], p53-W23L [t_R, 51.0 min; expected mass, 2298.2; observed mass, 2301.2 $(M + 2H)^{2+}$], p53-K24S [t_R, 51.6 min; expected mass, 2330.1; observed mass, 2333.0 $(M + 2H)^{2+}$], p53-L26I [t_R, 48.3 min; expected mass, 2371.2; observed mass, 2374.2 $(M + 2H)^{2+}$], p53-P27S [t_R, 53.9 min; expected mass, 2361.1; observed mass, 2364.2 $(M + 2H)^{2+}$], $p53_{7-36}$ [t_R, 51.7 min; expected mass, 3504.7; observed mass, 3507.2 $(M + 2H)^{2+}$], $p53_{17-29}$ [t_R, 51.4 min; expected mass, 1631.8; observed mass, 1632.8 $(M + H)$], $p53_{17-29}$-P27S [t_R, 55.2 min; expected mass, 1621.8; observed mass, 1622.9 $(M + H)$], $p65_{532-551}$ [t_R, 51.2 min; expected mass, 2219.0; observed mass, 2221.4 $(M+2H)^{2+}$], and phosphorylated $p65_{532-551}$ [t_R, 49.1 min; expected mass, 2298.0; observed mass, 2298.4 $(M - 2H)^{2-}$].

The peptides 333 and p53-P27S used in circular dichroism (CD) and NMR experiments were alkylated on cysteine to prevent oxidative disulfide formation. Purified peptides were lyophilized and subsequently dissolved in 1 mL of 1 M phosphate buffer (pH 7.5) containing 1 mg/mL of 2-bromoacetamide. The reaction was allowed to proceed for 30 min at room temperature with intermittent vortexing. The solution was filtered, followed by reverse-phase HPLC on a linear gradient of 0−60% buffer B in buffer A over 60 min. Analytical data for the peptides: 333-acetamide [t_R, 51.1 min; expected mass, 2428.3; observed mass, 2431.2 $(M + 2H)^{2+}$] and p53-P27S-acetamide [t_R, 54.6 min; expected mass, 2418.2; observed mass, 2421.4 $(M + 2H)^{2+}$].

Fluorescein Labeling of Peptides. Purified peptides were lyophilized and subsequently dissolved in 200 μL of 100 mM phosphate buffer (pH 4.0). A total of 200 μL of 5-iodoacetimidofluoroscein (10 mg/mL in DMF) was added slowly to the solution containing the peptide with gentle vortexing during addition. The reaction was allowed to proceed for 15−30 min at room temperature. $p65_{532-551}$ and phosphorylated $p65_{532-551}$ were dissolved in 300 μL of 100 mM phosphate buffer (pH 10.0). A total of 200 μL of fluorescein isothiocyanate isomer I (7 mg/mL in DMF) was added to the peptide solution with vortexing, and the solution was allowed to react for 20−30 min at room temperature. The solution was filtered, followed by purification by reverse-phase HPLC on a linear gradient of 15−55% buffer B in buffer A over 60 min. 363f and p53-P27Sf were purified by reverse-phase HPLC on a linear gradient of 15−55% buffer B in buffer A over 60 min, followed by 55−100% buffer B in buffer A over 10 min. Analytical data for fluorescein-labeled peptides: 333f [t_R, 55.7 min; expected mass, 2758.4; observed mass, 2761.8 $(M + 2H)^{2+}$], 336f [t_R, 50.7 min; expected mass, 2453.2; observed mass, 2456.2 $(M + 2H)^{2+}$], 633f [t_R, 52.5 min; expected mass, 2725.3; observed mass, 2728.4 $(M + 2H)^{2+}$], 636f [t_R, 49.2 min; expected mass, 2420.1; observed mass, 2422.0 $(M + 2H)^{2+}$], 666f [t_R, 52.5 min; expected mass, 2303.1; observed mass, 2305.2 $(M + 2H)^{2+}$], 663f [t_R, 59.1 min; expected mass, 2608.3; observed mass, 2610.8 $(M + 2H)^{2+}$], 366f [t_R, 49.9 min; expected mass, 2336.2; observed mass, 2338.6 $(M + 2H)^{2+}$], 363f [t_R, 61.5 min; expected mass, 2641.4; observed mass, 2644.0 $(M + 2H)^{2+}$], p53-D21Af [t_R, 58.8 min; expected mass, 2714.4; observed mass, 2716.8 $(M + 2H)^{2+}$], p53-W23Lf [t_R, 58.9 min; expected mass, 2685.4; observed mass, 2688.0 $(M + 2H)^{2+}$], p53-K24Sf [t_R, 54.4 min; expected mass, 2717.3; observed mass, 2719.4 $(M + 2H)^{2+}$], p53-L26If [t_R, 51.1 min; expected mass, 2758.4; observed mass, 2761.0 $(M + 2H)^{2+}$], p53-P27Sf [t_R, 60.6 min; expected mass, 2748.4; observed mass, 2751.0 $(M + 2H)^{2+}$], $p53_{7-36}$-f [t_R, 59.1 min; expected mass, 3892.0; observed mass, 3896.1 $(M + 3H)^{3+}$], $p65_{532-551}$-f [t_R, 58.4 min; expected mass, 2608.4; observed mass, 2610.6 $(M + 2H)^{2+}$], and phosphorylated $p65_{532-551}$-f [t_R, 55.1 min; expected mass, 2687.4; observed mass, 2687.2 $(M - 2H)^{2-}$].

Fluorescence Polarization Assays. Proteins and fluorescein-labeled ligands were diluted in PBS (140 mM NaCl, 2.7 mM KCl, 10 mM K_2HPO_4, and 2 mM KH_2PO_4 at pH 7.4) containing 0.1 mM DTT and 0.04 mg/mL bovine serum albumin (BSA) (BioRad). Concentrations of the labeled peptides were determined by UV absorbance at 492 nm, using an extinction coefficient for fluorescein of 83 000. Two-fold serial dilutions of MDM2 or $hTAF_{II}31$ proteins to concentrations ranging from 0.00015 μM (p53-P27S) or 0.0024 μM (other ligands) to 30 μM for MDM2 and from 0.24 to 60 μM for $hTAF_{II}31$ were mixed with ligands, which were kept at final concentrations of 100 nM (for all peptides except 336, which was at 50 nM, and p53-P27S, which was at 5 nM), in 96-well flat-bottom black opaque plates (Costar) with 150 μL total volume per well. After 30 min of incubation at room temperature, the plates were read on a Perkin-Elmer Fusion plate reader in fluorescence polarization mode with a 485 nm fluorescein excitation filter and a 535 nm emission filter with polarizer. Data indicate the average of at least three independent trials. Error bars indicate standard error.

Dissociation constants (K_d) were determined by a nonlinear least-squares curve fit (KaleidaGraph 4.0) of the K_d to the fluorescence polarization, via a binding equation for 1:1 complex formation. Peptide−protein complexes with dissociation constants higher than 500 nM were fit to a simplified binding isotherm (eq 1), with p_{min} = polarization in the absence of protein, p_{max} = polarization at saturation,

and the data fit to calculate p_{max} and K_d

$$\text{polarization} = p_{min} + (p_{max} - p_{min})\left(\frac{1}{1 + K_d/[\text{protein}]_{total}}\right) \quad (1)$$

The peptides with calculated dissociation constants lower than 500 nM were analyzed via a quadratic binding equation (eq 2), with the data fit to calculate p_{max} and K_d

$$\text{polarization} = p_{min} + (p_{max} - p_{min})[[\text{ligand}]_{total} + [\text{protein}]_{total} + K_d - (([\text{ligand}]_{total} + [\text{protein}]_{total} + K_d)^2 - 4[\text{ligand}]_{total}[\text{protein}]_{total}])^{1/2}/[2[\text{ligand}]_{total}] \quad (2)$$

CD Spectroscopy. CD spectra were collected at 298 K on a Jasco J-810 spectropolarimeter in a 1 mm cell with 75 μM peptide in 5 mM phosphate buffer (pH 7.0) containing 25 mM KF in H_2O or 30% trifluoroethanol (TFE) in H_2O. Data are the average of at least three independent trials. Individual spectra were collected every nanometer with a bandwidth of 2 nm and an averaging time of 4 s with two or three accumulations. Data were background-corrected but were not smoothed. Error bars are shown and indicate standard error.

NMR Spectroscopy. Peptides were dissolved in 90% H_2O/10% D_2O containing 20 mM phosphate and 10 mM NaCl ($p53_{17-29}$ and $p53_{17-29}$-P27S) or 5 mM phosphate and 25 mM NaCl (333 or p53-P27S). The pH of the solution was adjusted to pH 6.0. NMR spectra were collected at 23 °C on a Brüker AVC 600 MHz NMR spectrometer equipped with a triple-resonance cryoprobe or a TXI triple-resonance probe. NMR samples were prepared as 0.2−2.0 mM solutions. Spectra were referenced with deuterated 3-trimethylsilylproprionate (TSP). One-dimensional spectra and total correlation spectroscopy (TOCSY) spectra were collected with water suppression using a w5 pulse sequence with *z* gradients. Nuclear Overhauser effect spectroscopy (NOESY) spectra were collected with watergate water suppression. TOCSY spectra were acquired with sweep widths of 7183 Hz in t_1 and t_2, 600 × 4096 complex data points, 8 scans per t_1 increment, a relaxation delay of 1.5 s, and a TOCSY mixing time of 60 ms. NOESY spectra were acquired with sweep widths of 7183 Hz in t_1 and t_2, 600 × 4096 complex data points, 16−32 scans per t_1 increment, a relaxation delay of 2.0 s, and a NOESY mixing time of 300 ms. ^{1}H-^{13}C heteronuclear single-quantum coherence (HSQC) spectra were acquired on samples with natural abundance ^{13}C, using sweep widths of 12073 and 6009 Hz in t_1 and t_2, respectively, 600 × 4096 complex data points, 16 scans per t_1 increment, and a relaxation delay of 2.0 s. Delays in the ^{1}H-^{13}C HSQC experiment were based on a 1-bond C−H coupling constant of 145 Hz. Residues were assigned via TOCSY spectra, and sequential residues were identified via nuclear Overhauser effects (NOEs) between $H_\alpha(i)$ and $H_N(i + 1)$.

RESULTS AND DISCUSSION

The molecular basis for specific recognition of FXXΦΦ motifs by MDM2 was examined using a series of chimeras of the ADs of p53, which binds MDM2 with high affinity, and p65, whose affinity for MDM2 has not been quantified but has been determined to be worse than that of p53 (*16*, *19*, *20*, *29*, *30*). The FXXΦΦ motifs of p53 (FSDLW) and p65 (FSALL) are similar, differing in a single contact residue (Trp23) plus one noncontact residue, which could contribute electrostatically to binding specificity or affinity. In contrast, the flanking sequences are nonhomologous, with similar patterns of polar and hydrophobic residues but lacking a single identical residue. The flanking sequences in FXXΦΦ motifs could provide specificity and/or increased affinity for the disparate targets, as is observed in LXXLL motifs (*38*−*42*). Considering the experimental definitions, we note that p53 and p65 differ at p53 residue 26 [Leu (p53) versus Ile (p65)], which contacts MDM2 but is defined in the experimental design herein as part of the C-terminal flanking sequence. Similarly, Thr18 (p53), defined herein as part of the N-terminal flanking sequence, is a critical residue to stabilize binding to MDM2 and $hTAF_{II}31$, apparently via an α-helix-stabilizing hydrogen bond with the side chain or with the backbone amide of Asp21 (*20*, *23*, *30*).

FIGURE 1: Sequences of the peptides used in this study. Nomenclature for p53−p65 chimeric peptides indicates the source of the N-terminal sequence (first number), the central FXXΦΦ segment (middle number), and the C-terminal segment (final number), with 3 indicating that the segment is derived from p53 and 6 indicating that the segment is derived from p65. Residues derived from p53 are indicated in red, and residues from p65 are indicated in blue. Single-site variants of peptides derived from p53 synthesized are indicated by the site and nature of the residue substitution. All peptides were acetylated on the N terminus, except $p65_{532-551}$ and phosphorylated $p65_{532-551}$, which were fluorescein-labeled on the N terminus. All peptides except those containing p65-derived C-terminal segments contain C-terminal amides. The free C-terminal carboxylic acid (−OH), as is present in full-length p65, is indicated. Peptides were labeled on the N terminus with fluorescein isothiocyanate ($p65_{532-551}$ and phosphorylated $p65_{532-551}$) or on the added cysteine residue with 5-iodoacetamidofluorescein (all other peptides, except $p53_{17-29}$ and $p53_{17-29}$-P27S). Phosphorylated $p65_{532-551}$ contained phosphoserine at residue 536 (bold green).

Analysis of MDM2 Binding to Chimeric Peptides Derived from p53 and p65. A series of chimeric peptides was synthesized, in which residues were derived from the AD sequences of the p53 and p65 FXXΦΦ motifs and the N- and C-terminal sequences to that motif (Figure 1). Homologous sequence lengths were used, with the sequence length based on the observation that a 19-residue sequence of p53 shows high affinity for MDM2 (*20*, *25*−*30*). Peptides

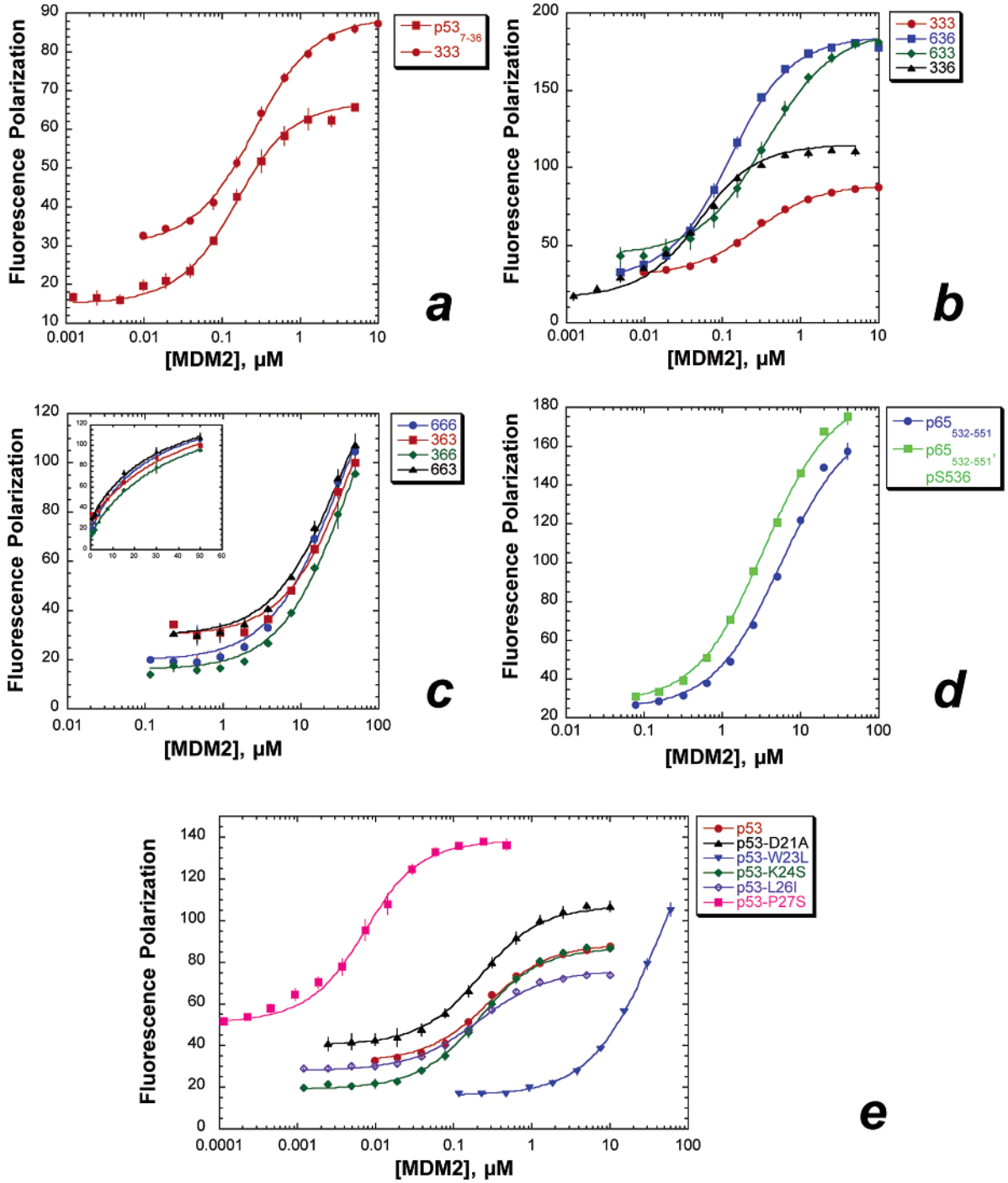

FIGURE 2: Fluorescence polarization data for $MDM2_{25-117}$ binding to peptides. Polarization data are in millipolarization units. Data represent the average of at least three independent trials. Error bars are shown and indicate standard error. (a) MDM2 binding to two different constructs of the p53 AD. (b) MDM2 binding to peptides containing the FXXΦΦ motif of p53. (c) MDM2 binding to peptides containing the FXXΦΦ motif of p65. (d) MDM2 binding to the extended p65 peptides $p65_{532-551}$ and $p65_{532-551}$ with Ser536 phosphorylated (pS536). (e) MDM2 binding to single-site variants of $p53_{12-30}$ (333).

containing extended sequences of the parent p53 and p65 peptides were also synthesized. In addition, a series of single-site substitution peptides was synthesized to analyze the roles of individual residues to binding specificity of MDM2. Peptides were labeled with fluorescein, and the binding to $MDM2_{25-117}$ was measured by fluorescence polarization.

Binding data (Figure 2 and Table 1) indicated that the central FSDLW motif of p53 is the critical recognition element for specific binding of p53 by MDM2. All chimeric peptides containing the FXXΦΦ motif (FSDLW) from p53 (X3X sequences) bound MDM2 with dissociation constants (K_d) <400 nM. In contrast, all chimeric peptides with the FXXΦΦ motif (FSALL) from p65 (X6X sequences) bound MDM2 with a K_d > 25 000 nM. These data indicate that MDM2 binds FSDLW with >2.6 kcal mol^{-1} specificity over FSALL.

The N-terminal ligand flanking sequence had a relatively small effect (<0.3 kcal mol^{-1} for most comparisons) on MDM2 specificity (e.g., 333 versus 633 or 366 versus 666) (parts a−d of Figure 2 and Table 1). The largest impact of the N-terminal sequence on MDM2 affinity was the N-terminal extension of p65-derived 666 to incorporate three

Table 1: $MDM2_{25-117}$ Binding Data to Peptides

peptide	K_d (μM)	error	ΔG^a (kcal mol^{-1})	$\Delta\Delta G^b$ (kcal mol^{-1})
$p53_{7-36}$	0.121	0.007	−9.4	−0.4
333 ($p53_{12-30}$)	0.229	0.012	−9.0	0.0[c]
336	0.036	0.002	−10.1	−1.1
633	0.353	0.013	−8.8	0.2
636	0.102	0.004	−9.5	−0.5
p53-D21A	0.170	0.007	−9.2	−0.2
p53-W23L	43	2	−6.0	3.0
p53-K24S	0.162	0.007	−9.2	−0.2
p53-L26I	0.209	0.014	−9.1	−0.1
p53-P27S	0.0047	0.0006	−11.3	−2.3
$p65_{532-551}$	5.7	0.2	−7.1	1.9
$p65_{532-551}$, pS536	3.4	0.1	−7.4	1.6
666	29	5	−6.2	2.8
663	33	5	−6.1	2.9
366	40	6	−6.0	3.0
363	49	14	−5.9	3.1

[a] ΔG indicates the free energy of binding and was calculated from $\Delta G = -RT\ln(1/K_d)$. [b] $\Delta\Delta G$ indicates the difference in the free energy of binding relative to the $MDM2_{25-117}$·$p53_{12-30}$ (333) complex. [c] $p65_{532-551}$, pS536 indicates the $p65_{532-551}$ peptide variant with Ser536 phosphorylated.

additional residues ($p65_{532-551}$), which improved binding by 0.9 kcal mol^{-1}, with an additional 0.4 kcal mol^{-1} improvement in affinity for MDM2 when this sequence is phosphorylated (Figure 2d). The increased affinity observed on N-terminal extension of p65-derived peptides is consistent with data that suggest that the binding of p65 to protein targets is increased by a second FXXΦΦ motif in p65 ($FSSIA_{538}$), which is present in the longer p65 peptide (*32*, *33*). In contrast to the results observed with p65-derived peptides, N- and C-terminal extension of p53-derived 333 [$p53_{12-30}$ (333) to $p53_{7-36}$] only modestly impacted binding to MDM2 (0.4 kcal mol^{-1}) (Figure 2a).

In contrast, the C-terminal flanking sequence more significantly impacted MDM2 binding than the N-terminal flanking sequence (parts b and c of Figure 2). Surprisingly, replacement of the p53 C-terminal sequence (333 or 633) with a p65 C-terminal sequence (336 or 636, respectively) *increased* the affinity of the p53−MDM2 interaction by 0.7−1.1 kcal mol^{-1}. A p53-derived sequence containing the p65 C-terminal flanking sequence (336) bound MDM2 with the highest affinity (K_d = 36 nM) among the swapped-domain chimeric peptides.

Effects of Single-Residue Modifications on MDM2 Affinity. The bases for MDM2 affinity and specificity were further analyzed with a series of single-site substitutions (Figure 2e and Table 1). Within a p53 context, individual residues from p53 were replaced with the corresponding residues from p65. Substitution of Asp21 with Ala (p53-D21A), from the FXXΦΦ motif, only minimally impacted MDM2 affinity, with a modest 0.2 kcal mol^{-1} improvement in binding observed. In combination with the minimal effect of p65-derived versus p53-derived N-terminal flanking sequences on MDM2 affinity, these data suggest that a hydrogen bond between Thr and the Asp21 side chain has little significance for p53−MDM2 affinity (*23*). Thr18 phosphorylation has been previously observed to significantly reduce the stability of the p53−MDM2 complex (*23*, *29*, *30*). Phosphorylation could disrupt an α-helical N-capping motif, between the Thr18 OH hydrogen-bond donor and the Asp21 carbonyl hydrogen-bond acceptor, observed crystallographically, by elimination of the Thr hydrogen-bond donor and additionally by electrostatic repulsion of the Asp and phosphothreonine side chains (*20*, *43*).

Trp23 is the key residue for specific recognition of p53 by MDM2 (*19*, *25*, *26*, *28*, *44*). Replacement of Trp23 with Leu, derived from p65, resulted in a 3.0 kcal mol^{-1} loss in binding affinity. Trp23 has been previously identified as a critical residue for MDM2 binding, and many functional analyses of Trp23 modification have been performed; however, the energetic importance of Trp23 to MDM2 binding has not been quantified experimentally (*19*, *25*, *26*, *28*, *44*). Trp23 is deeply buried in the p53−MDM2 crystal structures, contacting 10 residues of MDM2 (*20*, *42*). In addition, the Trp23 indole NH makes a hydrogen bond with the main-chain carbonyl of Leu54 of MDM2. Moreover, both the Phe19 and Leu26 side chains from p53 pack against Trp23, indicating that Phe19 and Leu26 may be important for organizing the Trp23 side chain to interact with MDM2 (*45*). In summary, these interactions are clearly critical for high-affinity binding to MDM2; however, modest MDM2 binding has been observed previously with a Trp23Ser substitution in p53 (*25*).

Surprisingly, p53-derived peptides with a C-terminal segment derived from p65 (e.g., 336 and 636) exhibited >1 kcal mol^{-1} greater affinity for MDM2 than was observed when a p53-derived C-terminal segment was present (e.g., 333 and 633). The bases for the increased MDM2 affinities of p53 variants with a p65-derived C-terminal flanking sequence were examined with p53 variants containing the single-residue substitutions K24S, L26I, or P27S. The free carboxy terminus in p65 is electrostatically similar to the Glu28 in p53 and seemed unlikely to explain the effect of the p65 C-terminal sequence on MDM2 affinity. The peptide p53-K24S modulates the electrostatics of complex formation, but K24 does not make hydrophobic contact with MDM2. The K24S modification did not significantly affect the stability of the complex (Figure 2e and Table 1). In contrast, Leu26 of p53 makes hydrophobic contact with Leu54, His96, and Ile99 of MDM2 and with Trp23 of p53, organizing the Trp side chain. However, analysis of the stability of the p53-L26I complex revealed that Leu and Ile at residue 26 contributed similarly to complex stability.

Replacement of Pro27 with p65-derived Ser resulted in a 2.3 kcal mol^{-1} increase in binding affinity. The observed binding constant (K_d = 4.7 nM) is the tightest measured affinity for a complex between MDM2 and a genetically encodable ligand and approaches the highest affinity (*46*, *47*) MDM2 ligands reported (*27*, *48*−*62*). Pro27 is conserved in all mammalian p53 sequences and is observed in a number of more distant p53 sequences, including *Xenopus laevis*. These data suggest a possible functional role of Pro27 in masking the FSDLW motif of p53, reducing the inherent affinity of the interaction of p53 with MDM2.

Characterization of the Structural Effects of Residue 27 Identity. To understand the molecular basis for the observed increased affinity of p53-P27S for MDM2, the peptides 333 and p53-P27S were examined by CD and NMR. CD spectra (Figure 3) indicated that p53-P27S was significantly more α-helical than 333, displaying an increase in mean residue ellipticity at 222 nm and a red shift in the minimum in the CD spectrum. The relatively small magnitude of the mean

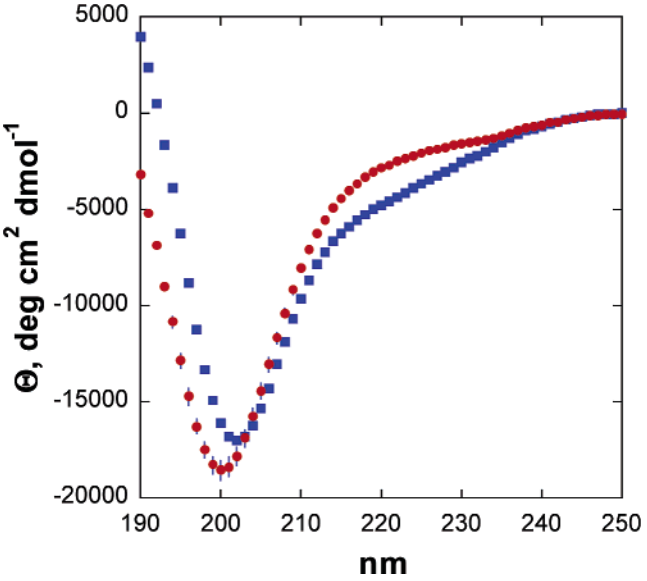

FIGURE 3: CD spectra of the peptides 333 ($p53_{12-30}$) (red circles) and p53-P27S (blue squares). Experiments were conducted at 25 °C in water containing 5 mM phosphate (pH 7.0) and 25 mM KF. Peptides were analyzed as the cysteine-alkylated acetamides.

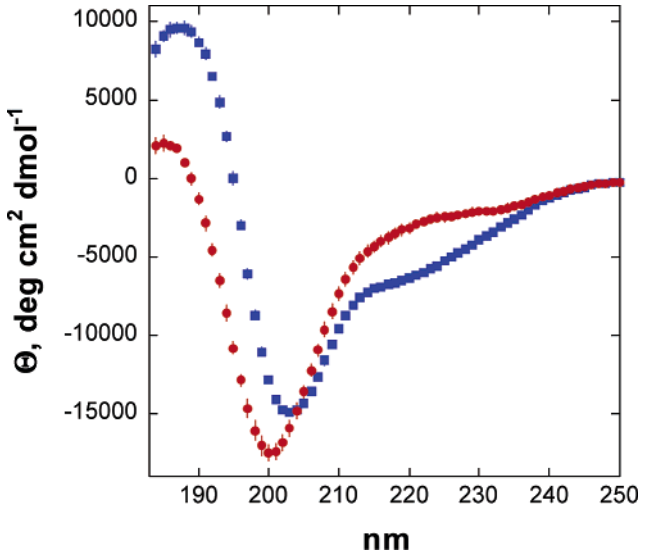

FIGURE 4: CD spectra of the peptides $p53_{17-29}$ (red circles) and $p53_{17-29}$-P27S (blue squares). Experiments were conducted at 25 °C in water containing 5 mM phosphate (pH 7.0) and 25 mM KF.

residue ellipticity at 222 nm even in p53-P27S reflects the observation that, in the p53−MDM2 complex, an α-helix is only observed over six residues (residues 19−24), only 30% of the sequence examined here.

To obtain further insight into the basis for the significantly higher MDM2 affinity of p53-P27S, two shorter peptides, $p53_{17-29}$ and $p53_{17-29}$-P27S, were synthesized for detailed analysis by CD and NMR. The smaller construct used for these experiments represents the sequence observed crystallographically to be well-ordered in the p53−MDM2 complex (*20*). The binding of a smaller construct, $p53_{9-25}$, to MDM2 and $hTAF_{II}31$ was also examined by Uesugi and Verdine (*19*). Moreover, previous work has shown that N-terminal truncation at residue 17 does not affect the stability of the p53−MDM2 complex (*29*, *30*).

$p53_{17-29}$-P27S was substantially more α-helical than $p53_{17-29}$ (Figure 4), as was observed in the longer peptides

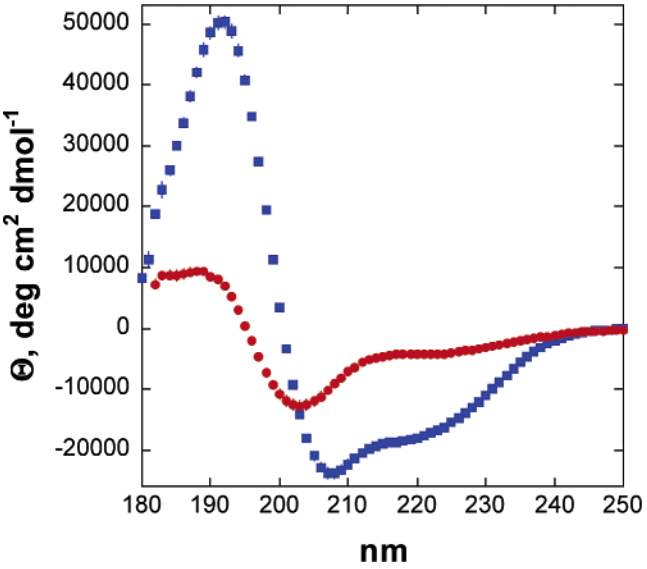

FIGURE 5: CD spectra of the peptides $p53_{17-29}$ (red circles) and $p53_{17-29}$-P27S (blue squares). Experiments were conducted at 25 °C in 30% TFE in water containing 5 mM phosphate (pH 7.0) and 25 mM KF. Note that the vertical axis in this figure is significantly different from that in Figure 4.

(Figure 3). An increase in α-helicity of $p53_{17-29}$-P27S is observable by a decrease in mean residue ellipticity at 222 nm, a red shift in the minimum near 200 nm, and the observation of an intense maximum in mean residue ellipticity near 190 nm. The difference in α helicity between $p53_{17-29}$ and $p53_{17-29}$-P27S is even more pronounced in 30% TFE, a strongly α-helix-promoting solvent (Figure 5) (*63*). $p53_{17-29}$-P27S exhibits a strong α-helical CD signature, with minima at 208 and 222 nm, a maximum at 192 nm, and greater than 50% α-helicity ($\Theta_{222} = -17\,170$ deg cm^2 dmol^{-1}). In contrast, even under strongly α-helix-promoting conditions (30% TFE), only weak α-helicity is observed for $p53_{17-29}$ ($\Theta_{222} = -4270$ deg cm^2 dmol^{-1}), indicating a significant energetic cost to forming an α-helix for the native p53 transactivation domain. When bound to MDM2, 6 of the 13 residues (46%) of $p53_{17-29}$ adopt an α-helix [Phe19−Leu24, with Leu25 additionally somewhat distorted from the α-helix ($\phi = -89°$, $\psi = +18°$); Leu26 and Pro27 adopt a polyproline helix conformation] (*20*). These data indicate that Pro27 substantially reduces the ability of the AD of p53 to adopt an α-helix, the observed MDM2-binding epitope.

The effects of P27S substitution on the structure of p53 were further examined by NMR (*24*, *64*−*66*). H_α and C_α chemical shifts correlate with protein secondary structure: H_α chemical shifts are more upfield in α-helices, whereas C_α chemical shifts are more downfield (*67*−*70*). A comparison of the H_α and C_α chemical shifts of $p53_{17-29}$ and $p53_{17-29}$-P27S (Figure 6 and Table 2) revealed that $p53_{17-29}$-P27S is significantly more α-helical than $p53_{17-29}$, consistent with the CD data. Increases in α-helicity were specifically observed in the MDM2-binding epitope, from Phe19−Leu26, with the largest changes in residues 23−26, which includes the critical MDM2 recognition residues Trp23 and Leu26. Of particular note is a dramatic change in the chemical shifts of Leu26, indicating a large conformational change from an extended or turn conformation to an α-helical conformation upon P27S substitution. In addition, chemical-shift index (CSI) analysis (Table 2) indicates an increase in the

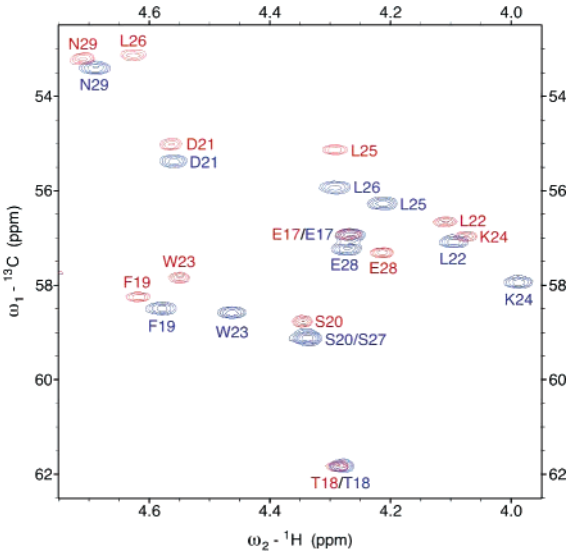

FIGURE 6: $H_\alpha-C_\alpha$ region of the ^{1}H-^{13}C HSQC spectra of $p53_{17-29}$ (red) and $p53_{17-29}$-P27S (blue). Data were collected at 296 K.

magnitude and extent of the α-helix for $p53_{17-29}$-P27S compared to $p53_{17-29}$ (*69*, *70*). Moreover, residues Leu22−Ser27 of $p53_{17-29}$-P27S all exhibited a three-bond coupling constant between the α proton and the amide proton ($^3J_{\alpha N}$) ≤6.1 Hz (see the Supporting Information), consistent with formation of a partial α-helix for these residues.

$p53_{17-29}$-P27S was further characterized by NOESY experiments at 277 K[2] (see the Supporting Information) (*24*, *64*). The observed NOE patterns were consistent with the adoption of a nascent α-helix by $p53_{17-29}$-P27S. Key NOEs were observed that are consistent with partial α-helix formation, including $H_\alpha(i)-H^N(i+1)$, $H_\alpha(i)-H^N(i+2)$, and $H_\alpha(i)-H^N(i+3)$ NOEs for Ser20, Asp21, Leu22, Trp23, and Lys24, as well as $H_\alpha(i)-H^N(i+4)$ NOEs for Ser20, Asp21, and Trp23. Also observed was a weak NOE between Trp23 H_β and Ser20 H_α; this NOE is consistent with a close contact observed between these atoms in the p53−MDM2 crystal structure. Moreover, although $p53_{17-29}$ exhibited the signature of a nascent α-helix, as was observed previously in NMR studies of p53 (*24*, *64*, *66*), a modestly reduced number of NOEs were observed in $p53_{17-29}$ compared to $p53_{17-29}$-P27S, with no $H_\alpha(i)-H^N(i+4)$ NOEs, generally weaker $H_\alpha(i)-H^N(i+3)$ NOEs, and no α-helical NOEs extending beyond Leu26 in $p53_{17-29}$. These data are consistent with the results above, indicating that $p53_{17-29}$-P27S is more α-helical than $p53_{17-29}$. Both peptides exhibited evidence of clustering of hydrophobic residues, as was observed previously for the p53 AD (*24*).

In summary, the NMR and CD data indicate that Pro27 reduces the stability of the recognition α-helix of p53, decreasing the population and stability of the functional MDM2-binding α-helical epitope. It has been previously observed that truncation of p53 after Leu26, or replacement of Pro27 with Tyr, resulted in an improvement in MDM2 binding of p53 peptides (*25*, *29*, *30*). In addition, none of the highest affinity peptide-based ligands for MDM2 retains Pro27 (*28*, *30*, *46*, *47*, *61*). However, examination of the p53−MDM2 crystal structure reveals no explanation for these observations; indeed, Pro27 makes hydrophobic contact with MDM2 (*20*). The data herein indicate that Pro27 significantly reduces the affinity of the p53−MDM2 interaction: replacement of Pro with Ser increases the affinity of the p53−MDM2 complex by 2.3 kcal mol^{-1}. These data suggest that Pro27 functions to stabilize the free, unbound form of the p53 AD in an inactive conformation by disrupting the α-helical recognition epitope, thereby reducing the energetic driving force for p53−MDM2 complex formation.

Several explanations for the reduced affinity of $p53_{17-29}$ compared to $p53_{17-29}$-P27S seem reasonable. First, proline may disrupt the α-helix because proline cannot provide an amide hydrogen to continue the hydrogen-bonding pattern characteristic of α-helices. Proline is a widely recognized α-helix termination signal (*71*). Indeed, in the p53−MDM2 structure, the last main-chain α-helical hydrogen bond is between the carbonyl of Leu22 and the amide of Leu26. Ser27 or other nonproline residues observed at this position in previously described high-affinity ligands could potentially stabilize the α-helix by hydrogen bonding to the Trp23 carbonyl (*20*).

Alternatively, an additional molecular basis to mask the p53 AD may be via the interaction of Pro27 with the aromatic residues Phe19 and Trp23 and/or the hydrophobic Leu residues. Interactions between aromatic residues and proline are particularly favorable, especially between tryptophan and proline, and would provide a strong energetic driving force for masking FSDLW (*72*, *73*). Interactions between Trp23 and Pro27 were observed in molecular dynamics simulations of $p53_{17-29}$ (*74*). Moreover, the proline-rich region of p53 is known to regulate and reduce the affinity of p53 for MDM2 via the interaction with the p53 AD (*75*−*78*). In addition, the proline-rich domain of p53 is a target for non-MDM2 protein−protein interactions (*79*−*85*). In combination with the data herein, these observations suggest that a possible role for proline residues and the proline-rich sequence of p53 may be to modulate the stability of the p53−MDM2 complex via tunable stabilization of the unbound form of p53 (*78*). The close proximity of the proline-rich domain and the AD in p53 is consistent with Pro27, and potentially other proline residues, being capable of interacting with FSDLW, providing tunable MDM2 affinity that is dependent upon the competitive interactions of the proline-rich domain with other proteins. Moreover, because proline-rich domains are common constituents of proteins important in cell signaling, proline-mediated intramolecular masking of protein recognition residues in disordered domains could potentially be a general mechanism of cellular regulation, analogous to other autoinhibitory regulatory mechanisms, such as those in protein kinases (*86*−*92*).

Determinants of Specificity in Binding $hTAF_{II}31$. The ADs of p53 and p65 interact with proteins in the general transcriptional machinery to activate transcription. One of these targets is the TFIID component $hTAF_{II}31$ (*17*, *19*, *21*−*23*, *25*, *93*−*95*). Binding of the p53 and p65 ADs to $hTAF_{II}$-31 is mediated by the short α-helical FXXΦΦ epitopes of p53 and p65 (*19*, *21*−*23*, *31*, *32*, *95*, *96*). The same FXXΦΦ motifs are used for both transcriptional activation and transcriptional repression, indicating that inhibitors of the p53−MDM2 interaction could potentially disrupt transcrip-

[2] A reduced number of NOEs were observed at 296 K, as expected for a dynamic structure; notably, the CD spectrum of $p53_{17-29}$-P27S was temperature-independent from 2 to 37 °C (see the Supporting Information).

Table 2: NMR-Derived Data for $p53_{17-29}$ and $p53_{17-29}$-P27S[a]

	$p53_{17-29}$				$p53_{17-29}$-P27S					
	δ, H_α	δ, C_α	H_α CSI	C_α CSI	δ, H_α	δ, C_α	H_α CSI	C_α CSI	$\Delta\delta$, H_α	$\Delta\delta$, C_α
Glu_{17}	4.26	56.9	−0.16	0.7	4.27	56.9	−0.15	0.7	0.01	0.0
Thr_{18}	4.28	61.8	−0.15	−0.2	4.28	61.8	−0.15	−0.2	0.00	0.0
Phe_{19}	4.61	58.2	−0.04	0.1	4.58	58.5	−0.07	0.4	−0.03	0.3
Ser_{20}	4.34	58.7	−0.17	0.0	4.34	59.1	−0.17	0.4	0.00	0.4
Asp_{21}	4.56	55.0	−0.26	2.0	4.56	55.3	−0.26	2.3	0.00	0.3
Leu_{22}	4.11	56.6	−0.27	1.1	4.10	57.1	−0.28	1.6	−0.01	0.5
Trp_{23}	4.54	57.8	−0.16	0.2	4.46	58.6	−0.24	1.0	−0.08	0.8
Lys_{24}	4.07	56.9	−0.29	0.2	3.99	57.9	−0.37	1.2	−0.08	1.0
Leu_{25}	4.29	55.1	−0.09	−0.4	4.22	56.2	−0.16	0.7	−0.07	1.1
Leu_{26}	4.63	53.1	+0.25	−2.4	4.29	55.9	−0.09	0.4	−0.34	2.8
Pro_{27}	4.38	63.7	−0.07	0.0	na	na	na	na	na	na
Ser_{27}	na	na	na	na	4.34	59.1	−0.17	0.4	na	na
Glu_{28}	4.21	57.3	−0.21	1.1	4.28	57.2	−0.14	1.0	0.07	−0.1
Asn_{29}	4.71	53.2	−0.08	−0.1	4.69	53.4	−0.10	0.1	−0.02	0.2

[a] Data were collected at 23 °C in 90% H_2O/10% D_2O with 20 mM phosphate (pH 6.5) and 10 mM NaCl. na = not applicable. CSI indicates the deviation from random-coil chemical-shift values (*69*, *70*). $\Delta\delta$ indicates the change in the indicated chemical shift (in ppm) in $p53_{17-29}$-P27S compared to $p53_{17-29}$: $\Delta\delta = \delta(p53_{17-29}\text{-P27S}) - \delta(p53_{17-29})$.

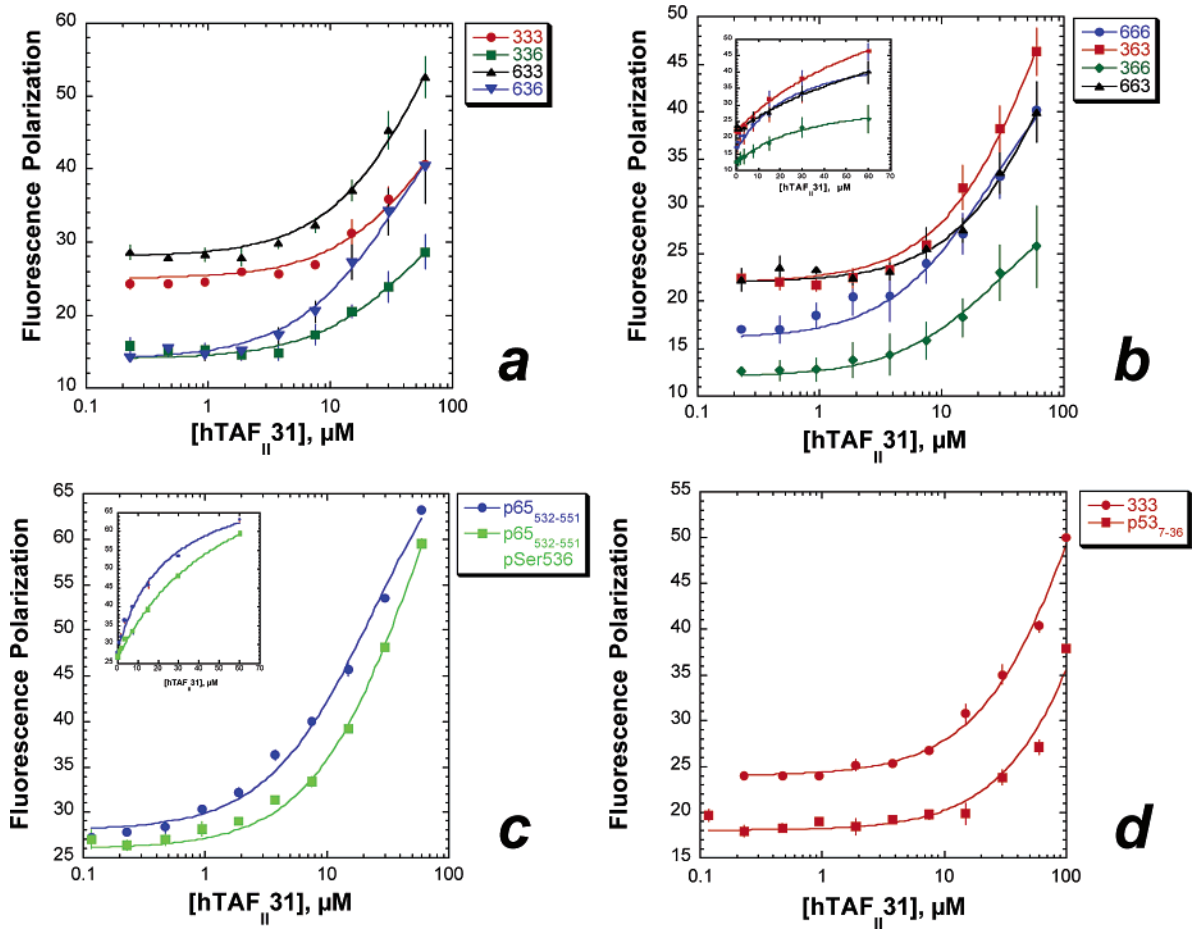

FIGURE 7: Fluorescence polarization data for $hTAF_{II}31_{1-140}$ binding to peptides. Polarization data are in millipolarization units. Data represent the average of at least three independent trials. Error bars are shown and indicate standard error. (a) $hTAF_{II}31_{1-140}$ binding to peptides containing the FXXΦΦ motif of p53. (b) $hTAF_{II}31_{1-140}$ binding to peptides containing the FXXΦΦ motif of p65. (c) $hTAF_{II}31_{1-140}$ binding to nonphosphorylated and phosphorylated $p65_{532-551}$ peptides. (d) $hTAF_{II}31_{1-140}$ binding to two different constructs of the p53 AD. Insets are shown on a linear scale of the protein concentration to indicate the extent to which saturation binding is approached.

tional activation as well. To address the determinants of specificity for transcriptional activation versus transcriptional repression, binding of the chimeric peptides to the N-terminal domain (residues 1−140) of $hTAF_{II}31$ was measured. $hTAF_{II}31_{1-140}$ was previously demonstrated to bind and induce α-helix formation in disparate ADs, including those of p53 and p65 (*19*, *21*−*23*, *95*).

Binding analysis (Figure 7 and Table 3) indicated that all peptides exhibited modest affinities to $hTAF_{II}31_{1-140}$. Although dissociation constants have not previously been measured for binding to $hTAF_{II}31_{1-140}$, the measured affinities are consistent with the data of Uesugi and Verdine, who estimated mid-to-high micromolar dissociation constants to $hTAF_{II}31_{1-140}$ based on NMR data (*19*, *21*). Among chimeric

Table 3: $hTAF_{II}31_{1-140}$ Binding Data to Peptides

peptide	K_d (μM)	error	ΔG^a (kcal mol^{-1})	$\Delta\Delta G^b$ (kcal mol^{-1})
$p53_{7-36}$	317	134	−4.8	1.4
333	163	44	−5.2	1.1
336	55	20	−5.8	0.4
633	78	21	−5.6	0.6
636	38	6	−6.0	0.2
p53-P27S	63	5	−5.7	0.5
$p65_{532-551}$	24	3	−6.3	−0.1
$p65_{532-551}$, pS536	55	8	−5.8	0.4
666	27	6	−6.2	0.0[c]
663	110	40	−5.4	0.8
366	33	5	−6.1	0.1
363	82	22	−5.6	0.7

[a] ΔG indicates the free energy of binding and was calculated from $\Delta G = -RT\ln(1/K_d)$. [b] $\Delta\Delta G$ indicates the difference in the free energy of binding relative to the $hTAF_{II}31_{1-140}$·$p65_{535-551}$ (666) complex. [c] $p65_{532-551}$, pS536 indicates the $p65_{532-551}$ peptide variant with Ser536 phosphorylated. The error indicates the calculated standard error of the curve fit.

peptides analyzed here, the lowest affinity for $hTAF_{II}31_{1-140}$ was exhibited by the extended p53 sequence ($p53_{7-36}$), which bound $hTAF_{II}31_{1-140}$ worse than 333. In general, peptides containing more p53-derived residues exhibited lower affinities for $hTAF_{II}31$ than the more p65-derived sequences, although the differences are modest in all cases. Notably, p53-P27S bound $hTAF_{II}31$ with only mid-micromolar affinity, indicating that p53-P27S exhibits very high specificity ($\Delta\Delta G = -5.6$ kcal mol^{-1}) for binding MDM2 over $hTAF_{II}31$ (Table 3 and the Supporting Information). Significant increases in binding specificity because of the stabilization of α-helical epitopes have been previously observed (*97*).

Phosphorylation of S536 did not increase the binding of $p65_{532-551}$ to $hTAF_{II}31_{1-140}$, in contrast to transcriptional activation data from cellular assays (*33*). Interestingly, $p65_{532-551}$ bound MDM2 with 0.8 kcal mol^{-1} greater affinity than $hTAF_{II}31_{1-140}$; phosphorylation of Ser536 further increased the preference of $p65_{532-551}$ for MDM2 by 0.8 kcal mol^{-1}, for a total of 1.6 kcal mol^{-1} specificity for MDM2 over $hTAF_{II}31_{1-140}$. These data indicate quantitatively how phosphorylation of the p65 AD may significantly impact its specificity for different binding partners (*23*, *29*, *30*).

The comparable $hTAF_{II}31_{1-140}$ binding affinities for most of the peptides herein is consistent with models of transcriptional activation in which hydrophobic and polar patches capable of adopting structured epitopes interact relatively nonspecifically with the general transcriptional machinery to initiate transcription (*1*, *3*, *5*, *10*, *15*, *19*, *22*, *25*, *32*, *41*, *98*−*105*). Under these models, specificity is to a significant extent provided spatially, via proximity and local concentration effects. Consistent with these models, it is noteworthy that, in solution, $p65_{532-551}$ binds MDM2 with significantly higher affinity than it binds $hTAF_{II}31_{1-140}$.

Transcriptional ADs are nonglobular hydrophobic protein segments that may bind to multiple cellular targets. Similarly, transcriptional co-activator and repressor proteins are conformationally plastic and hydrophobic proteins capable of binding to multiple targets (*86*−*88*, *106*, *107*). Biological function usually depends upon specificity in binding, under a given set of cellular conditions, to a limited subset of possible targets. Thermodynamic specificity is defined by differences in affinity to multiple possible targets and is inherently dependent upon the concentrations of all binding partners. Under a given set of conditions (e.g., higher protein concentration; see Figure 2 and consider [MDM2] = 10 μM, and [AD] ≤ 100 nM), multiple binding partners may be observed, whereas under more stringent conditions (e.g., [MDM2] = 100 nM, and [AD] ≤ 100 nM), binding to a more limited set of partners may be observed. Indeed, MDM2 was observed to effectively disrupt the $p65_{532-551}$·$hTAF_{II}31$ complex via the preferential binding of $p65_{532-551}$ to MDM2 (see the Supporting Information). In the current study, rigorous determination of binding constants was used to quantitatively address the determinants of thermodynamic specificity for binding partners in transcriptional activation and transcriptional repression.

FXXΦΦ motifs have been observed as common constituents of transcriptional ADs, which interact with the general transcriptional machinery to stimulate transcription (*19*, *21*, *22*, *108*). Because the FXXΦΦ motif of p53 also plays a critical regulatory role in binding to the repressor protein MDM2, we sought to understand the determinants for specific binding by MDM2, which, on the basis of previous data, apparently binds p53 as a specific target and is not an important regulator of other transcriptional ADs (e.g., p65) (*19*). Binding data from chimeric peptides revealed that most AD flanking residues contribute minimally to specific MDM2 binding. As the chimeric sequences were derived from ADs, the lack of sensitivity to the flanking sequence could be due to either general insensitivity to flanking sequences or functional similarity of the flanking sequences of different ADs.

Overexpression of MDM2 is observed in a number of human cancers. The data herein indicate that non-p53 transcriptional ADs bind MDM2 with low micromolar affinity, with the affinity tunable by phosphorylation of these proteins. These affinities are comparable to those measured for AD interactions with the transcriptional machinery (*2*−*5*, *109*). Under normal conditions, MDM2 binding to ADs could be largely prevented by the maintenance of low MDM2 concentrations in the cell. However, under conditions of MDM2 overexpression, MDM2 likely binds a variety of transcriptional ADs as targets, suggesting that other, non-p53-mediated transcription might be reduced under these conditions (*95*, *108*).

We have analyzed the determinants of specificity in recognition of the p53 and p65 ADs by the MDM2 repressor protein and the transcriptional machinery component $hTAF_{II}31$. Introduction of specificity is a critical challenge in the design of artificial activators and repressors (*4*, *10*, *92*, *103*, *109*−*114*). These results should be useful in the development of specific ligands for both MDM2 and $hTAF_{II}31$.

ACKNOWLEDGMENT

We thank Hua Lu for plasmids encoding full-length MDM2 and $hTAF_{II}31$. We thank Arlene Rockwell for preliminary experiments.

SUPPORTING INFORMATION AVAILABLE

Additional NMR, CD, and protein-binding data. This material is available free of charge via the Internet at http://pubs.acs.org.

REFERENCES

1. Ptashne, M., and Gann, A. (1997) Transcriptional activation by recruitment, *Nature 386*, 569−577.
2. Wu, Y., Reece, R. J., and Ptashne, M. (1996) Quantitation of putative activator−target affinities predicts transcriptional activating potentials, *EMBO J. 15*, 3951−3963.
3. Melcher, K. (2000) The strength of acidic activation domains correlates with their affinity for both transcriptional and non-transcriptional proteins, *J. Mol. Biol. 301*, 1097−1112.
4. Han, Y., and Kodadek, T. (2000) Peptides selected to bind the Ga180 repressor are potent transcriptional activation domains in yeast, *J. Biol. Chem. 275*, 14979−14984.
5. Wu, Z. Q., Belanger, G., Brennan, B. B., Lum, J. K., Minter, A. R., Rowe, S. P., Plachetka, A., Majmudar, C. Y., and Mapp, A. K. (2003) Targeting the transcriptional machinery with unique artificial transcriptional activators, *J. Am. Chem. Soc. 125*, 12390−12391.
6. Gaston, K., and Jayaraman, P. S. (2003) Transcriptional repression in eukaryotes: Repressors and repression mechanisms, *Cell. Mol. Life Sci. 60*, 721−741.
7. Oliner, J. D., Pietenpol, J. A., Thiagalingam, S., Gvuris, J., Kinzler, K. W., and Vogelstein, B. (1993) Oncoprotein MDM2 conceals the activation domain of tumor suppressor-p53, *Nature 362*, 857−860.
8. Momand, J., Wu, H.-H., and Dasgupta, G. (2000) MDM2−Master regulator of the p53 tumor suppressor protein, *Gene 242*, 15−29.
9. Moll, U. M., and Petrenko, O. (2003) The MDM2−p53 interaction, *Mol. Cancer Res. 1*, 1001−1008.
10. Majmudar, C. Y., and Mapp, A. K. (2005) Chemical approaches to transcriptional regulation, *Curr. Opin. Chem. Biol. 9*, 467−474.
11. Bargonetti, J., and Manfredi, J. J. (2002) Multiple roles of the tumor suppressor p53, *Curr. Opin. Oncol. 14*, 86−91.
12. Harris, S. L., and Levine, A. J. (2005) The p53 pathway: Positive and negative feedback loops, *Oncogene 24*, 2899−2908.
13. Chene, P. (2003) Inhibiting the p53−MDM2 interaction: An important target for cancer therapy, *Nat. Rev. Cancer 3*, 102−109.
14. Chene, P. (2004) Inhibition of the p53−MDM2 interaction: Targeting a protein−protein interface, *Mol. Cancer Res. 2*, 20−28.
15. Fischer, P. M. (2006) Peptide, peptidomimetic, and small-molecule antagonists of the p53−hDM2 protein−protein interaction, *Int. J. Pept. Res. Ther. 12*, 3−19.
16. Momand, J., Zambetti, G. P., Olson, D. C., George, D., and Levine, A. J. (1992) The MDM-2 oncogene product forms a complex with the p53 protein and inhibits p53-mediated transactivation, *Cell 69*, 1237−1245.
17. Lu, H., and Levine, A. J. (1995) Human $TAF_{II}31$ protein is a transcriptional coactivator of the p53 protein, *Proc. Natl. Acad. Sci. U.S.A. 92*, 5154−5158.
18. Lee, T. I., and Young, R. A. (1998) Regulation of gene expression by TBP-associated proteins, *Genes Dev. 12*, 1398−1408.
19. Uesugi, M., and Verdine, G. L. (1999) The α-helical FXXΦΦ motif in p53: TAF interaction and discrimination by MDM2, *Proc. Natl. Acad. Sci. U.S.A. 96*, 14801−14806.
20. Kussie, P. H., Gorina, S., Marechal, B. E., Moreau, J., Levine, A. J., and Pavletich, N. P. (1996) Structure of the MDM2 oncoprotein bound to the p53 tumor suppressor transactivation domain, *Science 274*, 948−952.
21. Uesugi, M., Nyanguile, O., Lu, H., Levine, A. J., and Verdine, G. L. (1997) Induced α helix in the VP16 activation domain upon binding to a human TAF, *Science 277*, 1310−1313.
22. Choi, Y., Asada, S., and Uesugi, M. (2000) Divergent $hTAF_{II}31$-binding motifs hidden in activation domains, *J. Biol. Chem. 275*, 15912−15916.
23. Jabbur, J. R., Tabor, A. D., Cheng, X. D., Wang, H., Uesugi, M., Lozano, G., and Zhang, W. (2002) MDM-2 binding and $TAF_{II}31$ recruitment is regulated by hydrogen bond disruption between the p53 residues Thr18 and Asp21, *Oncogene 21*, 7100−7113.
24. Botuyan, M. V. E., Momand, J., and Chen, Y. (1997) Solution conformation of an essential region of the p53 transactivation domain, *Folding Des. 2*, 331−342.
25. Lin, J. Y., Chen, J. D., Elenbaas, B., and Levine, A. J. (1994) Several hydrophobic amino acids in the p53 amino-terminal domain are required for transcriptional activation, binding to MDM-2 and the adenovirus-5 E1b 55-kD protein, *Genes Dev. 8*, 1235−1246.
26. Picksley, S. M., Vojtesek, B., Sparks, A., and Lane, D. P. (1994) Immunochemical analysis of the interaction of p53 with MDM2−Fine mapping of the MDM2 binding site on p53 using synthetic peptides, *Oncogene 9*, 2523−2529.
27. Bottger, V., Bottger, A., Howard, S. F., Picksley, S. M., Chene, P., GarciaEcheverria, C., Hochkeppel, H. K., and Lane, D. P. (1996) Identification of novel MDM2 binding peptides by phage display, *Oncogene 13*, 2141−2147.
28. Bottger, A., Bottger, V., GarciaEcheverria, C., Chene, P., Hochkeppel, H. K., Sampson, W., Ang, K., Howard, S. F., Picksley, S. M., and Lane, D. P. (1997) Molecular characterization of the hDM2−p53 interaction, *J. Mol. Biol. 269*, 744−756.
29. Lai, Z. H., Auger, K. R., Manubay, C. M., and Copeland, R. A. (2000) Thermodynamics of p53 binding to hDM2(1−126): Effects of phosphorylation and p53 peptide length, *Arch. Biochem. Biophys. 381*, 278−284.
30. Schon, O., Friedler, A., Bycroft, M., Freund, S. M. V., and Fersht, A. R. (2002) Molecular mechanism of the interaction between MDM2 and p53, *J. Mol. Biol. 323*, 491−501.
31. Giniger, E., and Ptashne, M. (1987) Transcription in yeast activated by a putative amphipathic α-helix linked to a DNA-binding unit, *Nature 330*, 670−672.
32. Schmitz, M. L., Silva, M. A. D., Altmann, H., Czisch, M., Holak, T. A., and Baeuerle, P. A. (1994) Structural and functional analysis of the NF-K-B p65 C-terminus−An acidic and modular transactivation domain with the potential to adopt an α-helical conformation, *J. Biol. Chem. 269*, 25613−25620.
33. Buss, H., Dorrie, A., Schmitz, M. L., Hoffmann, E., Resch, K., and Kracht, M. (2004) Constitutive and interleukin-1-inducible phosphorylation of p65 NF-KB at serine 536 is mediated by multiple protein kinases including IKB kinase (IKK)-α, IKKβ, IKKϵ, TRAF family member-associated (TANK)-binding kinase 1 (TBK1), and an unknown kinase and couples p65 to TATA-binding protein-associated factor II31-mediated interleukin-8 transcription, *J. Biol. Chem. 279*, 55633−55643.
34. Schmitz, M. L., Mattioli, I., Buss, H., and Kracht, M. (2004) NF-KB: A multifaceted transcription factor regulated at several levels, *ChemBioChem 5*, 1348−1358.
35. Zhao, L., and Chmielewski, J. (2005) Inhibiting protein−protein interactions using designed molecules, *Curr. Opin. Struct. Biol. 15*, 31−34.
36. Bond, G. L., Hu, W. W., and Levine, A. J. (2005) MDM2 is a central node in the p53 pathway: 12 years and counting, *Curr. Cancer Drug Targets 5*, 3−8.
37. Arkin, M. (2005) Protein−protein interactions and cancer: Small molecules going in for the kill, *Curr. Opin. Chem. Biol. 9*, 317−324.
38. Darimont, B. D., Wagner, R. L., Apriletti, J. W., Stallcup, M. R., Kushner, P. J., Baxter, J. D., Fletterick, R. J., and Yamamoto, K. R. (1998) Structure and specificity of nuclear receptor−coactivator interactions, *Genes Dev. 12*, 3343−3356.
39. McInerney, E. M., Rose, D. W., Flynn, S. E., Westin, S., Mullen, T.-M., Krones, A., Inostroza, J., Torchia, J., Nolte, R. T., Assa-Munt, N., Milburn, M. V., Glass, C. K., and Rosenfeld, M. G. (1998) Determinants of coactivator LXXLL motif specificity in nuclear receptor transcriptional activation, *Genes Dev. 12*, 3357−3368.
40. He, B., and Wilson, E. M. (2003) Electrostatic modulation in steroid receptor recruitment of LXXLL and FXXLF motifs, *Mol. Cell. Biol. 23*, 2135−2150.
41. Hermann, S., Berndt, K. D., and Wright, A. P. (2001) How transcriptional activators bind target proteins, *J. Biol. Chem. 276*, 40127−40132.
42. Ferreira, M. E., Hermann, S., Prochasson, P., Workman, J. L., Berndt, K. D., and Wright, A. P. H. (2005) Mechanism of transcription factor recruitment by acidic activators, *J. Biol. Chem. 280*, 21779−21784.
43. Aurora, R., and Rose, G. D. (1998) Helix capping, *Protein Sci. 7*, 21−38.
44. Massova, I., and Kollman, P. A. (1999) Computational alanine scanning to probe protein−protein interactions: A novel approach to evaluate binding free energies, *J. Am. Chem. Soc. 121*, 8133−8143.
45. Iqbalsyah, T. M., and Doig, A. J. (2005) Pairwise coupling in an Arg-Phe-Met triplet stabilizes α-helical peptide via shared rotamer preferences, *J. Am. Chem. Soc. 127*, 5002−5003.
46. Garcia-Echeverria, C., Chene, P., Blommers, M. J. J., and Furet, P. (2000) Discovery of potent antagonists of the interaction

between human double minute 2 and tumor suppressor p53, *J. Med. Chem. 43*, 3205−3208.
47. Zhang, R. M., Mayhood, T., Lipari, P., Wang, Y. L., Durkin, J., Syto, R., Gesell, J., McNemar, C., and Windsor, W. (2004) Fluorescence polarization assay and inhibitor design for MDM2/p53 interaction, *Anal. Biochem. 331*, 138−146.
48. Bottger, A., Bottger, V., Sparks, A., Liu, W. L., Howard, S. F., and Lane, D. P. (1997) Design of a synthetic MDM2-binding mini protein that activates the p53 response in vivo, *Curr. Biol. 7*, 860−869.
49. Stoll, R., Renner, C., Hansen, S., Palme, S., Klein, C., Belling, A., Zeslawski, W., Kamionka, M., Rehm, T., Muhlhahn, P., Schumacher, R., Hesse, F., Kaluza, B., Voelter, W., Engh, R. A., and Holak, T. A. (2001) Chalcone derivatives antagonize interactions between the human oncoprotein MDM2 and p53, *Biochemistry 40*, 336−344.
50. Zhao, J. H., Wang, M. J., Chen, J., Luo, A. P., Wang, X. Q., Wu, M., Yin, D. L., and Liu, Z. H. (2002) The initial evaluation of non-peptidic small-molecule hDM2 inhibitors based on p53−hDM2 complex structure, *Cancer Lett. 183*, 69−77.
51. Banerjee, R., Basu, G., Chene, P., and Roy, S. (2002) Aib-based peptide backbone as scaffolds for helical peptide mimics, *J. Pept. Res. 60*, 88−94.
52. Alluri, P. G., Reddy, M. M., Bachhawat-Sikder, K., Olivos, H. J., and Kodadek, T. (2003) Isolation of protein ligands from large peptoid libraries, *J. Am. Chem. Soc. 125*, 13995−14004.
53. Vassilev, L. T., Vu, B. T., Graves, B., Carvajal, D., Podlaski, F., Filipovic, Z., Kong, N., Kammlott, U., Lukacs, C., Klein, C., Fotouhi, N., and Liu, E. A. (2004) In vivo activation of the p53 pathway by small-molecule antagonists of MDM2, *Science 303*, 844−848.
54. Fasan, R., Dias, R. L. A., Moehle, K., Zerbe, O., Vrijbloed, J. W., Obrecht, D., and Robinson, J. A. (2004) Using a β-hairpin to mimic an α-helix: Cyclic peptidomimetic inhibitors of the p53−hDM2 protein−protein interaction, *Angew. Chem., Int. Ed. 43*, 2109−2112.
55. Kritzer, J. A., Lear, J. D., Hodsdon, M. E., and Schepartz, A. (2004) Helical β-peptide inhibitors of the p53−hDM2 interaction, *J. Am. Chem. Soc. 126*, 9468−9469.
56. Sakurai, K., Chung, H. S., and Kahne, D. (2004) Use of a retroinverso p53 peptide as an inhibitor of MDM2, *J. Am. Chem. Soc. 126*, 16288−16289.
57. Ding, K., Lu, Y., Nikolovska-Coleska, Z., Qiu, S., Ding, Y. S., Gao, W., Stuckey, J., Krajewski, K., Roller, P. P., Tomita, Y., Parrish, D. A., Deschamps, J. R., and Wang, S. M. (2005) Structure-based design of potent non-peptide MDM2 inhibitors, *J. Am. Chem. Soc. 127*, 10130−10131.
58. Grasberger, B. L., Lu, T. B., Schubert, C., Parks, D. J., Carver, T. E., Koblish, H. K., Cummings, M. D., LaFrance, L. V., Milkiewicz, K. L., Calvo, R. R., Maguire, D., Lattanze, J., Franks, C. F., Zhao, S. Y., Ramachandren, K., Bylebyl, G. R., Zhang, M., Manthey, C. L., Petrella, E. C., Pantoliano, M. W., Deckman, I. C., Spurlino, J. C., Maroney, A. C., Tomczuk, B. E., Molloy, C. J., and Bone, R. F. (2005) Discovery and cocrystal structure of benzodiazepinedione hDM2 antagonists that activate p53 in cells, *J. Med. Chem. 48*, 909−912.
59. Yin, H., Lee, G. I., Park, H. S., Payne, G. A., Rodriguez, J. M., Sebti, S. M., and Hamilton, A. D. (2005) Terphenyl-based helical mimetics that disrupt the p53/hDM2 interaction, *Angew. Chem., Int. Ed. 44*, 2704−2707.
60. Kritzer, J. A., Hodsdon, M. E., and Schepartz, A. (2005) Solution structure of a β-peptide ligand for hDM2, *J. Am. Chem. Soc. 127*, 4118−4119.
61. Kritzer, J. A., Zutshi, R., Cheah, M., Ran, F. A., Webman, R., Wongjirad, T. M., and Schepartz, A. (2006) Miniature protein inhibitors of the p53−hDM2 interaction, *ChemBioChem 7*, 29−31.
62. Hara, T., Durell, S. R., Myers, M. C., and Appella, D. H. (2006) Probing the structural requirements of peptoids that inhibit hDM2−p53 interactions, *J. Am. Chem. Soc. 128*, 1995−2004.
63. Cammers-Goodwin, A., Allen, T. J., Oslick, S. L., McClure, K. F., Lee, J. H., and Kemp, D. S. (1996) Mechanism of stabilization of helical conformations of polypeptides by water containing trifluoroethanol, *J. Am. Chem. Soc. 118*, 3082−3090.
64. Lee, H., Mok, K. H., Muhandiram, R., Park, K. H., Suk, J. E., Kim, D. H., Chang, J., Sung, Y. C., Choi, K. Y., and Han, K. H. (2000) Local structural elements in the mostly unstructured transcriptional activation domain of human p53, *J. Biol. Chem. 275*, 29426−29432.
65. Rosal, R., Pincus, M. R., Brandt-Rauf, P. W., Fine, R. L., Michl, J., and Wang, H. (2004) NMR solution structure of a peptide from the MDM-2 binding domain of the p53 protein that is selectively cytotoxic to cancer cells, *Biochemistry 43*, 1854−1861.
66. Vise, P. D., Baral, B., Latos, A. J., and Daughdrill, G. W. (2005) NMR chemical shift and relaxation measurements provide evidence for the coupled folding and binding of the p53 transactivation domain, *Nucleic Acids Res. 33*, 2061−2077.
67. Spera, S., and Bax, A. (1991) Empirical correlation between protein backbone conformation and Cα and Cβ ^{13}C nuclear magnetic resonance chemical shifts, *J. Am. Chem. Soc. 113*, 5490−5492.
68. Wishart, D. S., Sykes, B. D., and Richards, F. M. (1991) Relationship between nuclear magnetic resonance chemical shift and protein secondary structure, *J. Mol. Biol. 222*, 311−333.
69. Wishart, D. S., Sykes, B. D., and Richards, F. M. (1992) The chemical shift index: A fast and simple method for the assignment of protein secondary structure through NMR spectroscopy, *Biochemistry 31*, 1647−1651.
70. Wishart, D. S., and Sykes, B. D. (1994) The C-13 chemical shift index−A simple method for the identification of protein secondary structure using C-13 chemical-shift data, *J. Biomol. NMR 4*, 171−180.
71. Presta, L. G., and Rose, G. D. (1988) Helix signals in proteins, *Science 240*, 1632−1641.
72. Wu, W.-J., and Raleigh, D. P. (1998) Local control of peptide conformation: Stabilization of cis proline peptide bonds by aromatic proline interactions, *Biopolymers 45*, 381−394.
73. Thomas, K. M., Naduthambi, D., and Zondlo, N. J. (2006) Electronic control of amide cis−trans isomerism via the aromatic−prolyl interaction, *J. Am. Chem. Soc. 128*, 2216−2217.
74. Espinoza-Fonseca, L. M., and Trujillo-Ferrara, J. G. (2006) Transient stability of the helical pattern of region F19−L22 of the N-terminal domain of p53: A molecular dynamics simulation study, *Biochem. Biophys. Res. Commun. 343*, 110−116.
75. Walker, K. K., and Levine, A. J. (1996) Identification of a novel p53 functional domain that is necessary for efficient growth suppression, *Proc. Natl. Acad. Sci. U.S.A. 93*, 15335−15340.
76. Ruaro, E. M., Collavin, L., DelSal, G., Haffner, R., Oren, M., Levine, A. J., and Schneider, C. (1997) A proline-rich motif in p53 is required for transactivation-independent growth arrest as induced by Gas1, *Proc. Natl. Acad. Sci. U.S.A. 94*, 4675−4680.
77. Venot, C., Maratrat, M., Dureuil, C., Conseiller, E., Bracco, L., and Debussche, L. (1998) The requirement for the p53 proline-rich functional domain for mediation of apoptosis is correlated with specific PIG3 gene transactivation and with transcriptional repression, *EMBO J. 17*, 4668−4679.
78. Berger, M., Sionov, R. V., Levine, A. J., and Haupt, Y. (2001) A role for the polyproline domain of p53 in its regulation by MDM2, *J. Biol. Chem. 276*, 3785−3790.
79. Zhu, J. H., Zhou, W. J., Jiang, J. Y., and Chen, X. B. (1998) Identification of a novel p53 functional domain that is necessary for mediating apoptosis, *J. Biol. Chem. 273*, 13030−13036.
80. Zhu, J. H., Jiang, J. Y., Zhou, W. J., Zhu, K. C., and Chen, X. B. (1999) Differential regulation of cellular target genes by p53 devoid of the PXXP motifs with impaired apoptotic activity, *Oncogene 18*, 2149−2155.
81. Zhu, J., Zhang, S., Jiang, J., and Chen, X. (2000) Definition of the p53 functional domains necessary for inducing apoptosis, *J. Biol. Chem. 2000*, 39927−39934.
82. Jiang, M., Axe, T., Holgate, R., Rubbi, C. P., Okorokov, A. L., Mee, T., and Milner, J. (2001) p53 binds the nuclear matrix in normal cells: Binding involves the proline-rich domain of p53 and increases following genotoxic stress, *Oncogene 20*, 5449−5458.
83. Baptiste, N., Friedlander, P., Chen, X. B., and Prives, C. (2002) The proline-rich domain of p53 is required for cooperation with anti-neoplastic agents to promote apoptosis of tumor cells, *Oncogene 21*, 9−21.
84. Dornan, D., Shimizu, H., Burch, L., Smith, A. J., and Hupp, T. R. (2003) The proline repeat domain of p53 binds directly to the transcriptional coactivator p300 and allosterically controls DNA-dependent acetylation of p53, *Mol. Cell. Biol. 23*, 8846−8861.
85. Liu, G., Xia, T., and Chen, X. (2003) The activation domains, the proline-rich domain, and the C-terminal basic domain in p53 are necessary for acetylation of histones on the proximal p21 promoter and interaction with p300/CREB-binding protein, *J. Biol. Chem. 278*, 17557−17565.

86. Wright, P. E., and Dyson, H. J. (1999) Intrinsically unstructured proteins: Re-assessing the protein structure−function paradigm, *J. Mol. Biol. 293*, 321−331.
87. Dunker, A. K., Brown, C. J., Lawson, J. D., Iakoucheva, L. M., and Obradovic, Z. (2002) Intrinsic disorder and protein function, *Biochemistry 41*, 6573−6582.
88. Iakoucheva, L. M., Brown, C. J., Lawson, J. D., Obradovic, Z., and Dunker, A. K. (2002) Intrinsic disorder in cell-signaling and cancer-associated proteins, *J. Mol. Biol. 323*, 573−584.
89. Oldfield, C. J., Cheng, Y. G., Cortese, M. S., Romero, P., Uversky, V. N., and Dunker, A. K. (2005) Coupled folding and binding with α-helix-forming molecular recognition elements, *Biochemistry 44*, 12454−12470.
90. Moarefi, I., LaFevreBernt, M., Sicheri, F., Huse, M., Lee, C. H., Kuriyan, J., and Miller, W. T. (1997) Activation of the Src-family tyrosine kinase Hck by SH3 domain displacement, *Nature 385*, 650−653.
91. Nagar, B., Hantschel, O., Young, M. A., Scheffzek, K., Veach, D., Bornmann, V., Clarkson, B., Superti-Furga, G., and Kuriyan, J. (2003) Structural basis for the autoinhibition of c-Abl tyrosine kinase, *Cell 112*, 859−871.
92. Lu, Z., Rowe, S. P., Brennan, B. B., Davis, S. E., Metzler, R. E., Nau, J. J., Majmudar, C. Y., Mapp, A. K., and Ansari, A. Z. (2005) Unraveling the mechanism of a potent transcriptional activator, *J. Biol. Chem. 280*, 29689−29698.
93. Sauer, F., Hansen, S. K., and Tjian, R. (1995) Multiple TAF_{II}s directing synergistic activation of transcription, *Science 270*, 1783−1788.
94. Farmer, G., Colgan, J., Nakatani, Y., Manley, J. L., and Prives, C. (1996) Functional interaction between p53, the TATA-binding protein (TBP), and TBP-associated factors in vivo, *Mol. Cell. Biol. 16*, 4295−4304.
95. Buschmann, T., Lin, Y. H., Aithmitti, N., Fuchs, S. Y., Lu, H., Resnick-Silverman, L., Manfredi, J. J., Ronai, Z., and Wu, X. W. (2001) Stabilization and activation of p53 by the coactivator protein $TAF_{II}31$, *J. Biol. Chem. 276*, 13852−13857.
96. Ansari, A. Z., Mapp, A. K., Nguyen, D. H., Dervan, P. B., and Ptashne, M. (2001) Towards a minimal motif for artificial transcriptional activators, *Chem. Biol. 8*, 583−592.
97. Zondlo, N. J., and Schepartz, A. (1999) Highly specific DNA recognition by a designed miniature protein, *J. Am. Chem. Soc. 121*, 6938−6939.
98. Regier, J. L., Shen, F., and Triezenberg, S. J. (1993) Pattern of aromatic and hydrophobic amino acids critical for one of 2 subdomains of the VP16 transcriptional activator, *Proc. Natl. Acad. Sci. U.S.A. 90*, 883−887.
99. Cress, W. D., and Triezenberg, S. J. (1991) Critical structural elements of the VP16 transcriptional activation domain, *Science 251*, 87−90.
100. Arora, P. S., Ansari, A. Z., Best, T. P., Ptashne, M., and Dervan, P. B. (2002) Design of artificial transcriptional activators with rigid poly-L-proline linkers, *J. Am. Chem. Soc. 124*, 13067−13071.
101. Minter, A. R., Brennan, B. B., and Mapp, A. K. (2004) A small molecule transcriptional activation domain, *J. Am. Chem. Soc. 126*, 10504−10505.
102. Buhrlage, S. J., Brennan, B. B., Minter, A. R., and Mapp, A. K. (2005) Stereochemical promiscuity in artificial transcriptional activators, *J. Am. Chem. Soc. 127*, 12456−12457.
103. Majmudar, C. Y., Lum, J. K., Prasov, L., and Mapp, A. K. (2005) Functional specificity of artificial transcriptional activators, *Chem. Biol. 12*, 313−321.
104. Lum, J. K., and Mapp, A. K. (2005) Artificial transcriptional activation domains, *ChemBioChem 6*, 1311−1315.
105. Taatjes, D. J., Marr, M. T., and Tjian, R. (2004) Opinion−Regulatory diversity among metazoan co-activator complexes, *Nat. Rev. Mol. Cell. Biol. 5*, 403−410.
106. Schon, O., Friedler, A., Freund, S., and Fersht, A. R. (2004) Binding of p53-derived ligands to MDM2 induces a variety of long range conformational changes, *J. Mol. Biol. 336*, 197−202.
107. Liu, J., Perumal, N. B., Oldfield, C. J., Su, E. W., Uversky, V. N., and Dunker, A. K. (2006) Intrinsic disorder in transcription factors, *Biochemistry 45*, 6873−6888.
108. Chi, S. W., Lee, S. H., Kim, D. H., Ahn, M. J., Kim, J. S., Woo, J. Y., Torizawa, T., Kainosho, M., and Han, K. H. (2005) Structural details on MDM2−p53 interaction, *J. Biol. Chem. 280*, 38795−38802.
109. Frangioni, J. V., LaRiccia, L. M., Cantley, L. C., and Montminy, M. R. (2000) Minimal activators that bind to the KIX domain of p300/CBP identified by phage display screening, *Nat. Biotechnol. 18*, 1080−1085.
110. Parker, D., Rivera, M., Zor, T., Henrion-Caude, A., Radhakrishnan, I., Kumar, A., Shapiro, L. H., Wright, P. E., Montminy, M., and Brindle, P. K. (1999) Role of secondary structure in discrimination between constitutive and inducible activators, *Mol. Cell. Biol. 19*, 5601−5607.
111. Shimogawa, H., Kwon, Y., Mao, Q., Kawazoe, Y., Choi, Y., Asada, S., Kigoshi, H., and Uesugi, M. (2004) A wrench-shaped synthetic molecule that modulates a transcription factor−coactivator interaction, *J. Am. Chem. Soc. 126*, 3461−3471.
112. Best, J. L., Amezcua, C. A., Mayr, B., Flechner, L., Murawsky, C. M., Emerson, B., Zor, T., Gardner, K. H., and Montminy, M. (2004) Identification of small-molecule antagonists that inhibit an activator−coactivator interaction, *Proc. Natl. Acad. Sci. U.S.A. 101*, 17622−17627.
113. Volkman, H. M., Rutledge, S. E., and Schepartz, A. (2005) Binding mode and transcriptional activation potential of high affinity ligands for the CBPKIX domain, *J. Am. Chem. Soc. 127*, 4649−4658.
114. Liu, B., Alluri, P. G., Yu, P., and Kodadek, T. (2005) A potent transactivation domain mimic with activity in living cells, *J. Am. Chem. Soc. 127*, 8254−8255.

BI060309G